Physica E 75 (2016) 93–96

Contents lists available at ScienceDirect

Physica E

journal homepage: www.elsevier.com/locate/physe

Electromagnetically induced transparency in a cascade-type quantum well subband system under intense picosecond excitation

S. Hanna [a], B. Eichenberg [a], D.A. Firsov [b], L.E. Vorobjev [b], V.M. Ustinov [c], A. Seilmeier [a,*]

[a] Physikalisches Institut, Universität Bayreuth, D-95440 Bayreuth, Germany
[b] Peter the Great St. Petersburg Polytechnic University, St. Petersburg 195251, Russia
[c] Ioffe Physico-Technical Institute, St. Petersburg 194021, Russia

ARTICLE INFO

Article history:
Received 19 August 2015
Accepted 8 September 2015
Available online 10 September 2015

Keywords:
Coherent effects
EIT
Intersubband transition
Time resolved spectroscopy

ABSTRACT

The coherent light–matter interaction in a 4-level cascade-type subband system of an asymmetric GaAs/AlGaAs quantum well structure is studied in pump-probe transmission experiments with picosecond (ps) time resolution. Coupling two excited subbands by an intense mid-infrared laser pulse at low sample temperatures is found to result in a substantially increased transparency of the fundamental e_1–e_2 transition. We find a reduction of the absorption coefficient by ~80%, which is one of the most pronounced electromagnetically induced transparency in solid state systems observed so far.

1. Introduction

In atomic vapors, which have long dephasing times, matter–wave interference effects resulting in electromagnetically induced transparency (EIT) or gain without inversion have been extensively explored [1,2]. In solid media, however, these effects are much more difficult to observe due to the considerably reduced dephasing times.

Semiconductor quantum well (QW) structures represent a class of artificial composite materials suitable for experiments on EIT in solids [3] owing to their large intersubband transition matrix element in the midinfrared (MIR) of a few nanometers, which results in fairly high Rabi frequencies Ω at moderate light intensities (~200 MW/cm^{-2}) that are still below any damage threshold. Furthermore, transition frequencies and absorption strengths can be tailored within a wide range, which makes these structures interesting for practical applications.

This paper presents time and spectrally resolved data that show quantum interference in a QW sample with four coupled electronic subbands and demonstrate EIT experimentally. Time and spectrally resolved studies of intersubband transitions are not only versatile tools for the investigation of the incoherent population dynamics within a subband system, but they also provide a probe to access coherent interaction processes.

First experiments on EIT and gain without inversion in quantum well structures have been reported in [4,5]. In this work, however, the applied pulse widths are not in the order of 100 ps, but only about 2 ps. Furthermore, both time and spectrally resolved data demonstrating quantum coherence and interference effects will be presented.

2. Experiment

2.1. Experimental setup

The coherent bleaching dynamics following the intense optical excitation of the quantum well (QW) sample, which has been cooled down to a 20 K temperature, is studied time and spectrally resolved in an MIR/MIR pump-probe transmission experiment with a picosecond time resolution.

For the experimental investigations a laser system is utilized that generates two single MIR laser pulses via difference frequency generation between the emission of a flash lamp-pumped actively and passively mode-locked Nd:glass laser at 1.053 μm and the near-infrared emission of two traveling-wave dye lasers [6]. The single pulses can be accurately time delayed with respect to each other and are independently and continuously tunable in their wavelengths in the spectral range from 4–12 μm. They exhibit pulse durations (FWHM) of approximately 2 ps, spectral widths (FWHM) of 1.6–1.9 meV, and single pulse energies in the order of 1 μJ. A low 8 Hz repetition rate of both pump and probe pulses ensures that thermal equilibrium is reached in the sample after every laser shot.

A schematic of the experimental setup is shown in Fig. 1. For the sample, a prism-reflection geometry is chosen with a 63° internal angle of incidence between the normal of the QW layer and

* Corresponding author.

http://dx.doi.org/10.1016/j.physe.2015.09.012
1386-9477/

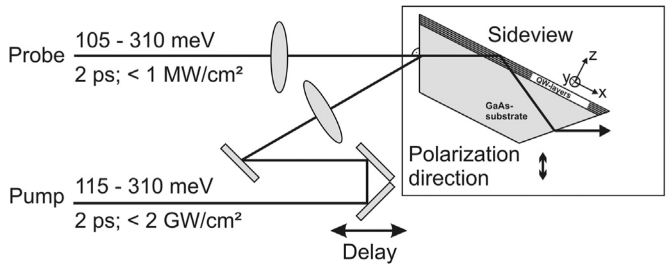

Fig. 1. Schematic of the pump-probe experiment. The pump and probe pulses are independently tunable between 105 and 310 meV. Inset: 63° wedge of the QW sample including the optical path of probe transmission.

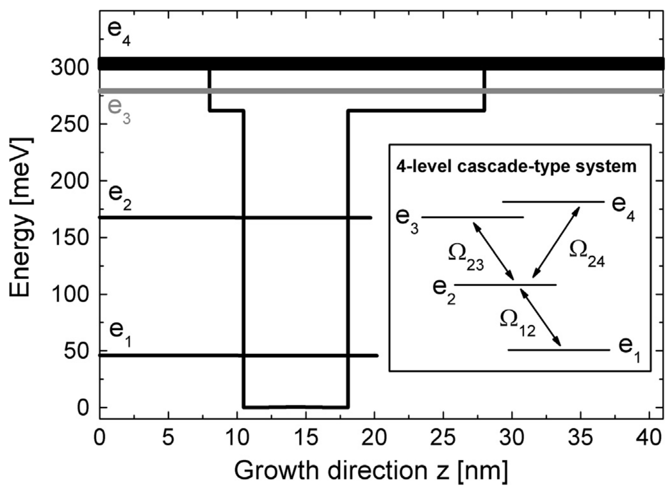

Fig. 2. Single quantum well band structure in the conduction band at a 300 K lattice temperature. Four electronic subbands e_i are calculated in a single particle picture that takes into account the band nonparabolicity in growth direction as well as the subband splitting. Inset: Schematics of the 4-level cascade-type subband system under study. The bound electronic subbands depicted in Fig. 2 are coupled at Rabi frequencies Ω_{nm} by the driving electric fields.

the pump and probe beams. Whereas the probe beam is normally incident to the sample's entrance facet, the pump beam hits that interface at an approximately 30° angle with respect to the normal of the surface. The polarization direction of both beams is shown in Fig. 2.

2.2. Sample structure

The investigated sample is a GaAs/$Al_xGa_{1-x}As$ multiple quantum well (MQW) structure, grown by molecular beam epitaxy on a semi-insulating GaAs substrate. The MQW layer consists of 60 asymmetric funnel-shaped quantum wells separated by 8 nm thick $Al_{0.4}Ga_{0.6}As$ barriers. They are embedded between two 200 nm wide $Al_xGa_{1-x}As$ gradient layers (x=0.9…0.4) with the Al concentration decreasing towards the MQW stack.

Fig. 2 shows the band structure of one of the QWs in the conduction band which consists of a 7.6 nm wide Silicon n-doped GaAs layer between 2.5 nm and 9.9 nm wide $Al_{0.35}Ga_{0.65}As$ layers. The doping in the wells with a $2.6\times10^{17}\ \text{cm}^{-3}$ concentration is kept fairly modest. The bound electron levels, e_i, are calculated using the envelope function approach in the effective mass approximation as applied to heterostructures [7].

Due to the comparatively large barrier thickness, the subband splitting is negligible for the lower two states: the calculated single particle subband energies are 46.0 meV and 167.6 meV with respect to the GaAs band edge at 300 K for the e_1 and e_2 electronic subbands, respectively. However, because of the effectively reduced barrier width, owing to the structural asymmetry and the resulting increased interaction with neighboring quantum wells, the e_3 and e_4 subbands at center energies of 279.3 meV and 305.5 meV are split into 1.7 meV and 8.8 meV wide mini-bands, respectively. The oscillator strengths calculated for the e_1–e_2-, e_2–e_3- and e_2–e_4 intersubband transitions are $f_{12}=0.9$, $f_{23}=0.5$ and $f_{24}=0.7$.

3. Results and discussion

At a sample temperature of 300 K, only the e_1–e_2 absorption band shows up in a Fourier transform infrared (FTIR) spectrum at a photon energy of 121.8 meV, which coincides with the calculated transition frequency (121.6 meV). Decreasing the temperature to 20 K, the e_1–e_2 absorption band shifts blue to a 123.5 meV band center energy, exhibiting a Lorentzian lineshape of only 6.8 meV spectral width (FWHM), cf. Fig. 3. From the doping concentration of $2.6\times10^{17}\ \text{cm}^{-3}$ a Fermi level of ~54 meV is estimated, which leaves higher subbands unoccupied. Consequently, transitions between upper subbands are not observed. According to the envelope function calculations, the e_2–e_3 and e_2–e_4 resonances are expected to occur at 113.6 meV and 139.8 meV at 20 K, respectively.

3.1. Incoherent population dynamics

In order to study the incoherent population dynamics, the sample is first excited within the fundamental e_1–e_2 intersubband transition at a $\hbar\omega=122.7$ meV photon energy (see Fig. 3).

The excitation intensity corresponds to a Rabi energy of $\Omega_{12}=\mu E/\hbar\sim19$ meV. (μ is the transition dipole moment and E is the electric field of the excitation pulse) By means of the excitation, the ground state e_1 is partially depopulated and states in the initially virtually unpopulated first excited state e_2 are filled. Therefore, a bleaching $-\Delta A=\ln\frac{T(t_d)}{T_0}>0$ of the fundamental transition is observed by a second tunable probe pulse at longer pump-probe delay times t_d, with $T(t_d)$ denoting the intensity transmitted through the sample. T_0 is the sample transmission without excitation. The absorption is nearly completely bleached at short delay times of a few ps. The bleaching signal that decays with a time constant of 5 ps is shifted to lower frequencies due to multiparticle effects. The increased electron density in the e_2

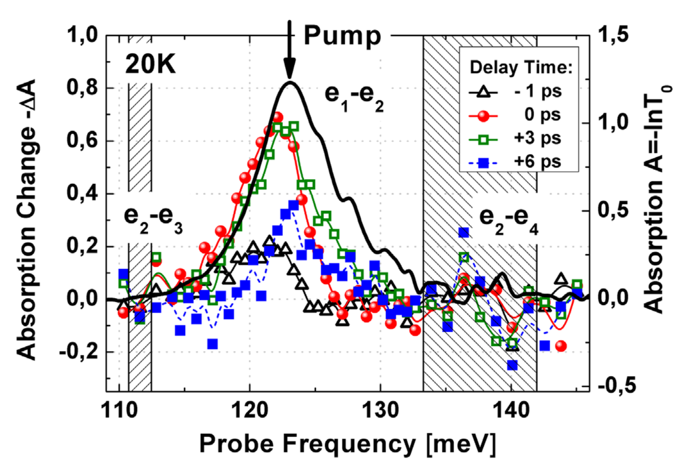

Fig. 3. Transient bleaching signal (data points, left axis) within the e_1–e_2 intersubband absorption band (solid line, right axis) after excitation resonantly at $\hbar\omega=123.5$ meV (vertical arrow) with a Rabi frequency $\Omega_{12}\sim19$ meV. The excitation of the fundamental transition depopulates the ground subband e_1 and populates the first excited subband e_2, which leads to the expected incoherent bleaching of the e_1–e_2 transition. Shaded areas: Calculated frequency bands of the e_2–e_3 and e_2–e_4 intersubband transitions.